Available online at www.sciencedirect.com
ScienceDirect
International Journal of Heat and Mass Transfer 49 (2006) 4987–5000
International Journal of HEAT and MASS TRANSFER
www.elsevier.com/locate/ijhmt

Conjugate natural convection heat transfer in an inclined square cavity containing a conducting block

Manab Kumar Das *, K. Saran Kumar Reddy [1]

Department of Mechanical Engineering, Indian Institute of Technology Guwahati, North Guwahati, Guwahati 781039, Assam, India

Received 28 October 2005; received in revised form 2 May 2006
Available online 22 August 2006

Abstract

The present work is concerned with computation of natural convection flow in a square enclosure with a centered internal conducting square block both of which are given an inclination angle. Finite volume method through the concepts of staggered grid and SIMPLE algorithm have been applied. Deferred QUICK scheme has been used to discretize the convective fluxes and central difference for diffusive fluxes. The problem of conjugate natural convection has been taken up for validating the code. The abrupt variation in the properties at the solid/fluid interface are taken care of with the harmonic mean formulation. Solution has been performed in the computational domain as a whole with proper treatment at the solid/fluid interface. Computations have been performed for $Ra = 10^3$–10^6, angle of inclination varying from 15° to 90° in steps of 15° and ratio of solid to fluid thermal conductivities of 0.2 and 5.0. Results are presented in terms of streamlines, isotherms, local and average Nusselt number.
© 2006 Elsevier Ltd. All rights reserved.

Keywords: Natural convection; Conjugate heat transfer; Numerical simulation

1. Introduction

Over the past years, natural convection process has been studied by various researchers because of its relevance to heat transfer in many science and engineering applications. Natural convection heat transfer is relevant to large scale natural phenomena in the fields of astrophysics, geophysics, atmospheric sciences, and a wide range of engineering applications such as cooling of electronic equipment, solidification processes, growing crystals and solar collectors. These are always complex interactions between the finite fluid content inside the enclosure with the enclosure walls. Since the velocity and the temperature equations are coupled due to the buoyancy force, the study of natural convection is very complex.

A large number of research articles are available which deal with the study of natural convection in simple geometry enclosures with either vertical or horizontal imposed heat flux or temperature difference. A thorough review work can be obtained in Ostrach [1]. Conjugate heat transfer with natural convection is an important area because it changes the boundary conditions as well as the heat transfer processes. Kim and Viskanta [2] studied the effect of solid wall on the differentially heated cavity. They considered different cases where heating was done from top, side and bottom wall of a square cavity. They concluded that Nusselt number depends not only on the flow but also on the thermal and geometrical parameters of the walls enclosing the cavity.

de Vahl Davis [3] has presented a numerical solution of natural convection in a differentially heated square cavity where the top and the bottom surfaces are maintained adiabatic whereas the vertical surfaces are differentially heated. This problem generally is used as the benchmark situation for validating a computer code. Modification of this problem to include the conjugate heat transfer or complicated

* Corresponding author. Tel.: +91 361 2582655; fax: +91 361 2690762.
E-mail addresses: manab@iitg.ernet.in (Manab Kumar Das), saranreddy123@yahoo.co.in (K. Saran Kumar Reddy).
[1] Present address: Tata Motors, Pune, India.

0017-9310/$ - see front matter © 2006 Elsevier Ltd. All rights reserved.
doi:10.1016/j.ijheatmasstransfer.2006.05.041

Nomenclature

g	acceleration due to gravity
h	convection coefficient
k	thermal conductivity of the fluid
k_s	thermal conductivity of the solid
k^*	thermal conductivity ratio of solid to fluid
L	length of enclosure
Nu	Nusselt number
p	dimensionless pressure
Pr	Prandtl number
Ra	Rayleigh number
S, *Source*	source term
T	dimensionless temperature
u, v	dimensionless velocity components in x- and y-directions
W	size of the body
x, y	dimensionless Cartesian coordinates

Greek symbols

α	thermal diffusivity
α_p	under-relaxation parameter
β	coefficient of thermal expansion
ζ	dimensionless body size
ρ	density
ν	kinematic viscosity
ϕ	angle of inclination
φ	general variable

Subscripts

avg	average
c	cold surface
e, w, n, s	control volume faces
h	hot surface
L	local
max	maximum
nb	neighbouring grid point
∞	ambient conditions

Superscript

*	guessed value/dimensional variable

cavity problem has been solved and presented in literatures. House et al. [4] have investigated the effect of a centered conducting body on natural convection in an enclosure. The effect of Rayleigh number, Prandtl number, body size, ratio of thermal conductivities are studied. The important observation made is that the heat transfer across the enclosure, in comparison to that in the absence of a body, may be enhanced (reduced) by a body with a thermal conductivity ratio less (greater) than unity. This is an important observation as far as conjugate heat transfer is concerned. Sathe and Joshi [5] studied the natural convection arising from a heat generating substrate-mounted protrusion in an enclosure. The boundaries are maintained at isothermal cold conditions. They concluded that in actual situation, substrate conduction effects cannot be neglected. Also, it may be inappropriate to prescribe simple boundary conditions such as constant temperature or heat flux on the protrusion faces and solve for the governing equations only in the fluid.

Sun and Amery [6] considered the effect of a heat source and an internal baffle on natural convection heat transfer in a rectangular enclosure. All the walls are of finite conductance. The horizontal walls are considered to be adiabatic on the boundary whereas the vertical walls are differentially heated. They also concluded that it is inappropriate to specify simple boundary conditions on the walls and to neglect the conduction through the baffles. The complete conjugate heat conduction, convection and radiation problem for a heated block in a differentially heated square enclosure is solved by Liu and Phan-Tien [7]. The boundary conditions of the enclosure is similar to that of de Vahl Davis [3]. In comparison to the problem considered by House et al. [4], the block is generating heat. The conduction and the emission of the block has a substantial effect on the heat transfer situation. Ha and Jung [8] conducted a numerical study of conjugate heat transfer of natural convection in a cubic enclosure with a centered cubic heat-conducting heat generating body. Right and left vertical walls are maintained at differentially heated condition. All other walls are insulated. The presence of the solid body results in a larger variation of the local Nusselt number compared to cases without a cubic conducting body in the enclosure.

Yucel and Ozdem [9] studied natural convection in a square enclosure with partial dividers. The top and bottom walls are maintained adiabatic or perfectly conducting while the left and right walls are maintained at differential temperature. They observed that there is definite variation of the mean Nusselt number with the Rayleigh number and the number and the size of partitions. Ha et al. [10] carried out two-dimensional unsteady natural convection inside an enclosure with a square body. The bottom wall is hot and the top wall is cold. Four different thermal boundary condition of the square body is considered: cold isothermal body, neutral isothermal body, hot isothermal body and adiabatic body. They reported an unsteady flow and temperature fields when the Rayleigh number is high. It also depends upon the thermal boundary condition of the body.

It is observed that the study of natural convection of an inclined cavity in the presence of an inclined conducting block has not been carried out so far. The influence of the angle of inclination is studied here with the view to know the effect of angle, on the heat transfer characteristics. In the present case, the various parameters considered are $Ra = 10^3$–10^6, angle of inclination from 15° to 90° and two k^* viz. 0.2 and 5.0.

2. Description of the problem

The geometry being solved here is that of an inclined square enclosure with sides of length L (Fig. 1). The cold wall ($T_c = 0.0$) is making an angle of ϕ with horizontal direction. For $\phi = 0°$, cold wall becomes the bottom wall whereas for $\phi = 90°$, it becomes the right vertical wall. Opposite to the cold wall ($T_c = 0$) is the hot wall ($T_h = 1.0$). Other two walls are maintained at adiabatic condition. The solid conducting body centered at $\frac{L}{2}$, has sides of length W with thermal conductivity k_s. The flow within the enclosure is laminar and gravitational acceleration acts parallel to the walls. Boussinesq approximation is assumed to be valid and the problem is formulated as a steady state case.

3. Governing equations and boundary conditions

Natural convection is governed by the differential equations expressing the conservation of mass, momentum, and energy. The present flow is considered steady, laminar, incompressible and two-dimensional. The viscous dissipation term in the energy equation is neglected. The momentum equations are simplified using Boussinesq approximation, in which all fluid properties are assumed constant except the density in its contribution to the buoyancy force. The governing equations and the boundary conditions are cast in dimensionless form using the following dimensionless variables:

$$x = \frac{x^*}{L},\quad y = \frac{y^*}{L},\quad u = \frac{u^* L}{\alpha},\quad v = \frac{v^* L}{\alpha},\quad p = \frac{p^* L^2}{\rho \alpha^2},\quad \zeta = \frac{W}{L}$$

$$\alpha = \frac{k}{\rho C_p},\quad k^* = \frac{k_s}{k_f},\quad Nu = \frac{hL}{k},\quad Ra = \frac{g\beta \Delta T^* L^3}{v\alpha},\quad T = \frac{T^* - T_c^*}{\Delta T^*}$$

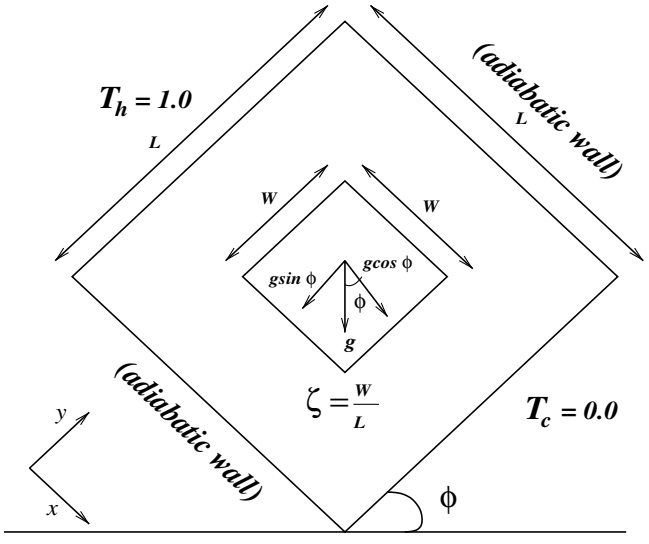

Fig. 1. Schematic diagram of tilted cavity and the solid body.

Continuity equation:

$$\frac{\partial u}{\partial x} + \frac{\partial v}{\partial y} = 0 \tag{1}$$

x-Momentum equation:

$$\frac{\partial (u^2)}{\partial x} + \frac{\partial (uv)}{\partial y} = -\frac{\partial p}{\partial x} + Pr\left(\frac{\partial^2 u}{\partial x^2} + \frac{\partial^2 u}{\partial y^2}\right) - RaPrT\cos\phi \tag{2}$$

y-Momentum equation:

$$\frac{\partial (uv)}{\partial x} + \frac{\partial v^2}{\partial y} = -\frac{\partial p}{\partial y} + Pr\left(\frac{\partial^2 v}{\partial x^2} + \frac{\partial^2 v}{\partial y^2}\right) + RaPrT\sin\phi \tag{3}$$

Energy equation in fluid:

$$\frac{\partial (uT)}{\partial x} + \frac{\partial (vT)}{\partial y} = \left(\frac{\partial^2 T}{\partial x^2} + \frac{\partial^2 T}{\partial y^2}\right) \tag{4}$$

Energy equation in the solid:

$$\frac{\partial \left(k^* \frac{\partial T}{\partial x}\right)}{\partial x} + \frac{\partial \left(k^* \frac{\partial T}{\partial y}\right)}{\partial y} = 0 \tag{5}$$

where k^* is the ratio of thermal conductivity of the body to that of the fluid.

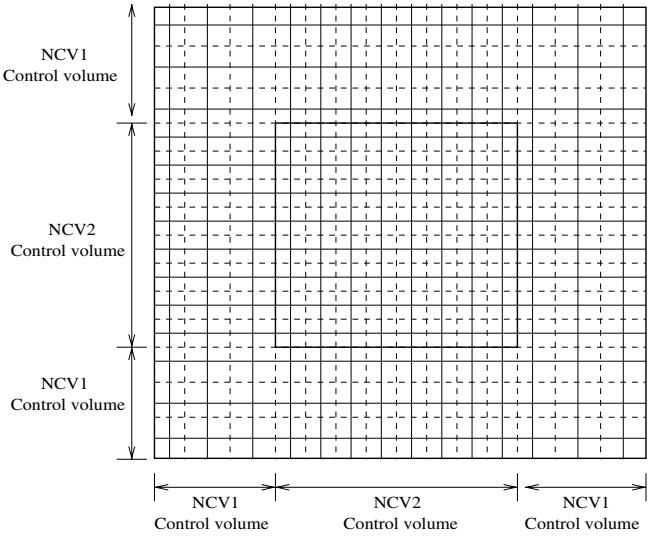

Fig. 2. The computational grid with NCV1 and NCV2 control volumes.

Table 1
Grid independence study

NCV1	NCV2	Nu_{avg}
Case (a): $Ra = 10^5$ and $k^* = 5.0$		
22	20	4.31698
27	25	4.31046
30	28	4.30800
Case (b): $Ra = 10^5$ and $k^* = 0.2$		
22	20	4.63162
27	25	4.62404
30	28	4.62117

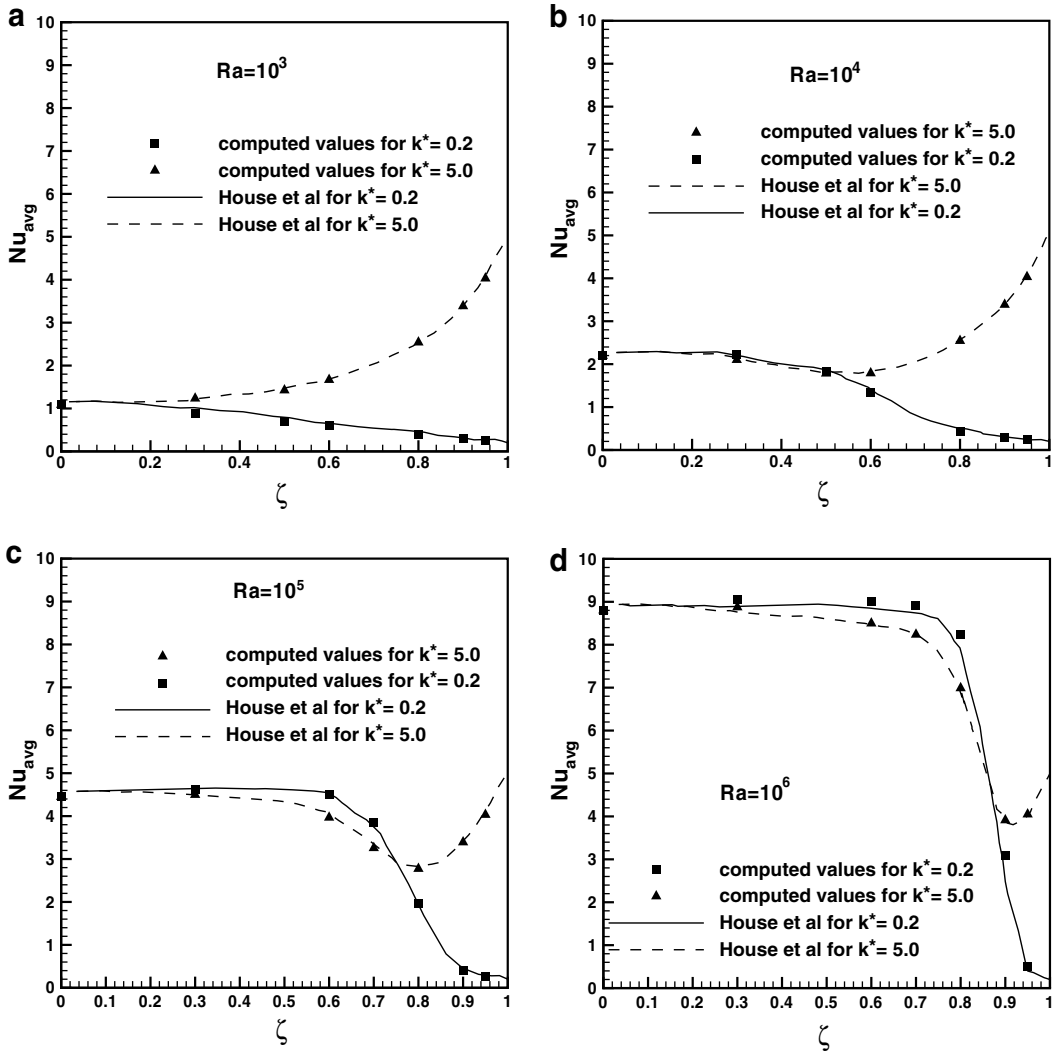

Fig. 3. The effect of ζ on average Nusselt number for different Rayleigh numbers and thermal conductivity ratios (k^*) for (a) $Ra = 10^3$, (b) $Ra = 10^4$, (c) $Ra = 10^5$, (d) $Ra = 10^6$.

The boundary conditions used in the problem are

1. At $x = 0$, $0 \leqslant y \leqslant 1$, $T = 1.0$.
2. At $x = 1$, $0 \leqslant y \leqslant 1$, $T = 0.0$.
3. At $y = 0$ and at $y = 1.0$, $0 \leqslant x \leqslant 1$, $\frac{\partial T}{\partial y} = 0.0$.
4. On all sides of the body, $T_s = T_f$ and $\frac{\partial T}{\partial n}\big|_f = k^* \frac{\partial T}{\partial n}\big|_s$.

The angle of inclination of the block and enclosure is varied from 15° to 90° with increments of 15°.

4. Numerical procedure

Numerical solution of the governing equations is done by finite volume method, using SIMPLE algorithm as given in Patankar [11] on a staggered grid. Deferred QUICK scheme of Hayase et al. [12] was used in discretizing the convective fluxes in the interior points and deferred central difference was used in discretizing the convective fluxes for the points adjacent to the boundaries. The generalized equations resulting from the finite volume discretization will be of the form

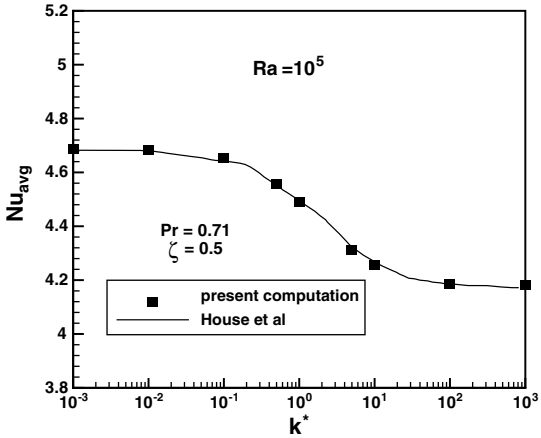

Fig. 4. The variation of average Nusselt number with k^* for Rayleigh number 10^5 and $\zeta = 0.5$.

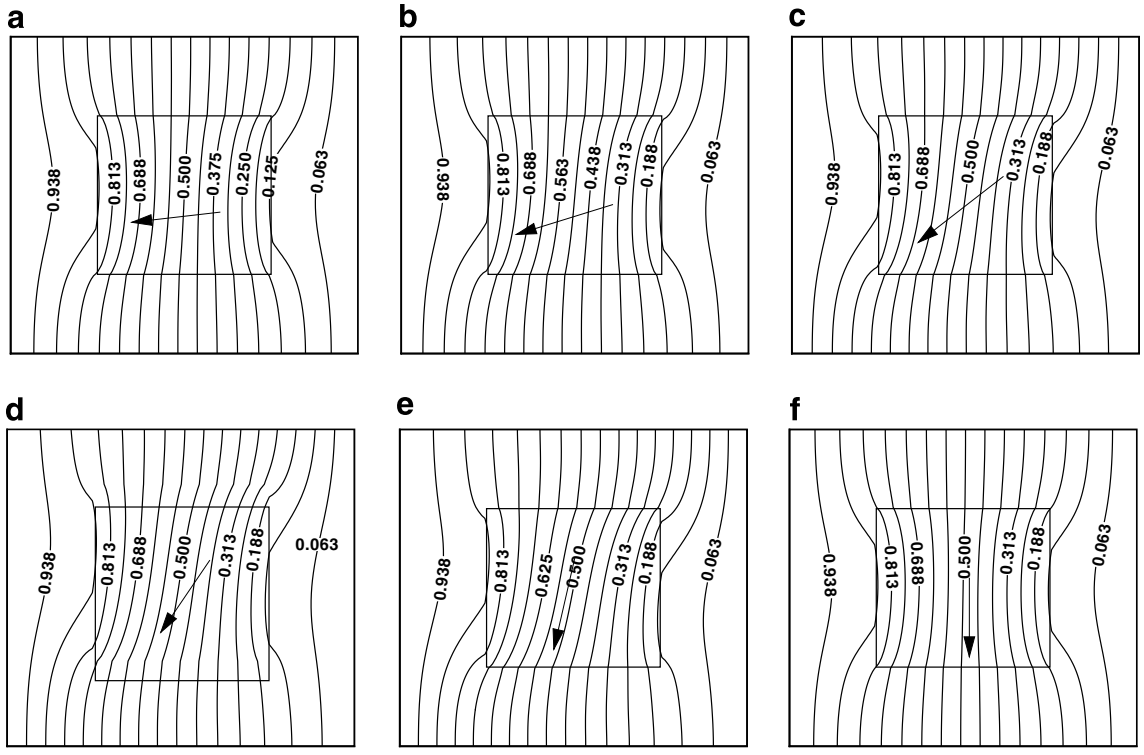

Fig. 5. The various isotherm plots for $Ra = 10^3$, $\zeta = 0.5$ and $k^* = 0.2$ beginning with an angle of inclination of 15° and in increments of 15°.

$$a_P\varphi_P = a_E\varphi_E + a_W\varphi_W + a_N\varphi_N + a_S\varphi_S + \text{source}^{\varphi}(x,y) = \sum a_{\text{nb}}\varphi_{\text{nb}} + \text{source}^{\varphi}(x,y) \quad (6)$$

where $a_P = a_E + a_W + a_N + a_S + a_0$.

In the present formulation the computational domain was divided into control volumes such that the control volume faces fall on the boundary of the square body. The equations are solved in the fluid and the solid regions

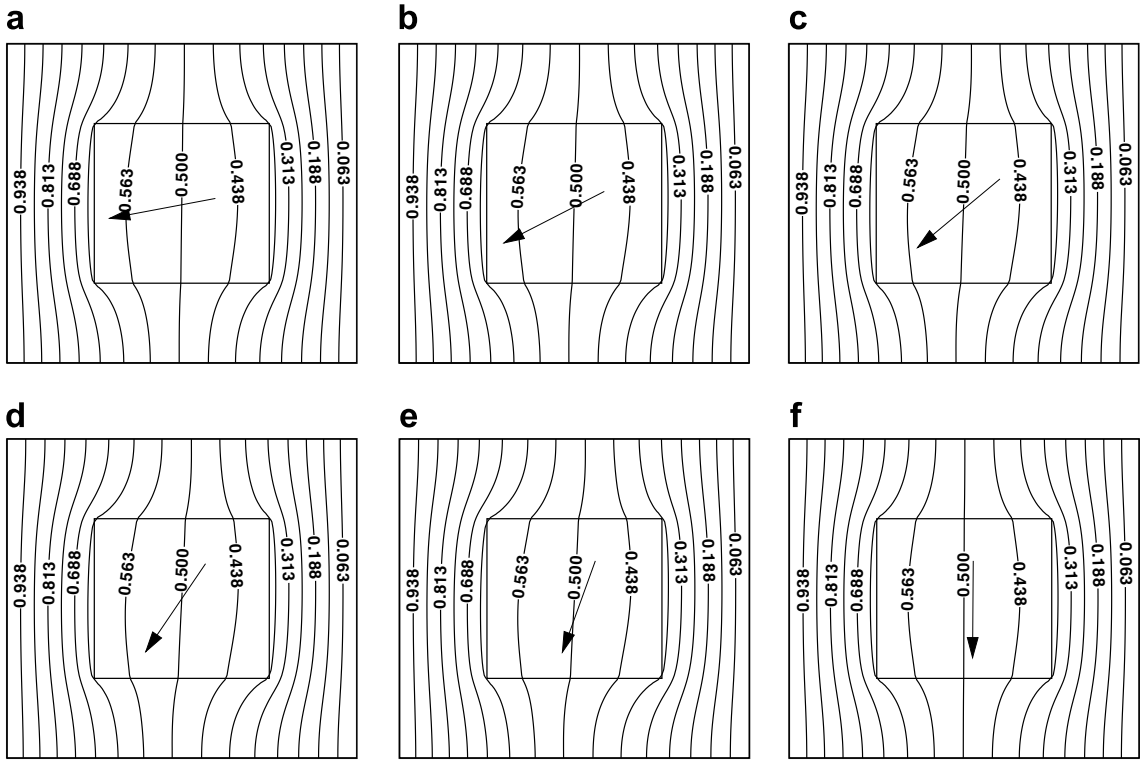

Fig. 6. The various isotherm plots for $Ra = 10^3$, $\zeta = 0.5$ and $k^* = 5.0$ beginning with an angle of inclination of 15° and in increments of 15°.

simultaneously with suitable modifications. In the fluid region the momentum equations are solved as usual and when the solid medium is reached the velocities in the solid region were made zero using the following procedure.

To the coefficient a_P a large value of the order 10^{30} is added. The actual values of a_P and other coefficients being small compared with the numerical value added, make the value of the property φ_P to zero. The property φ_P used in

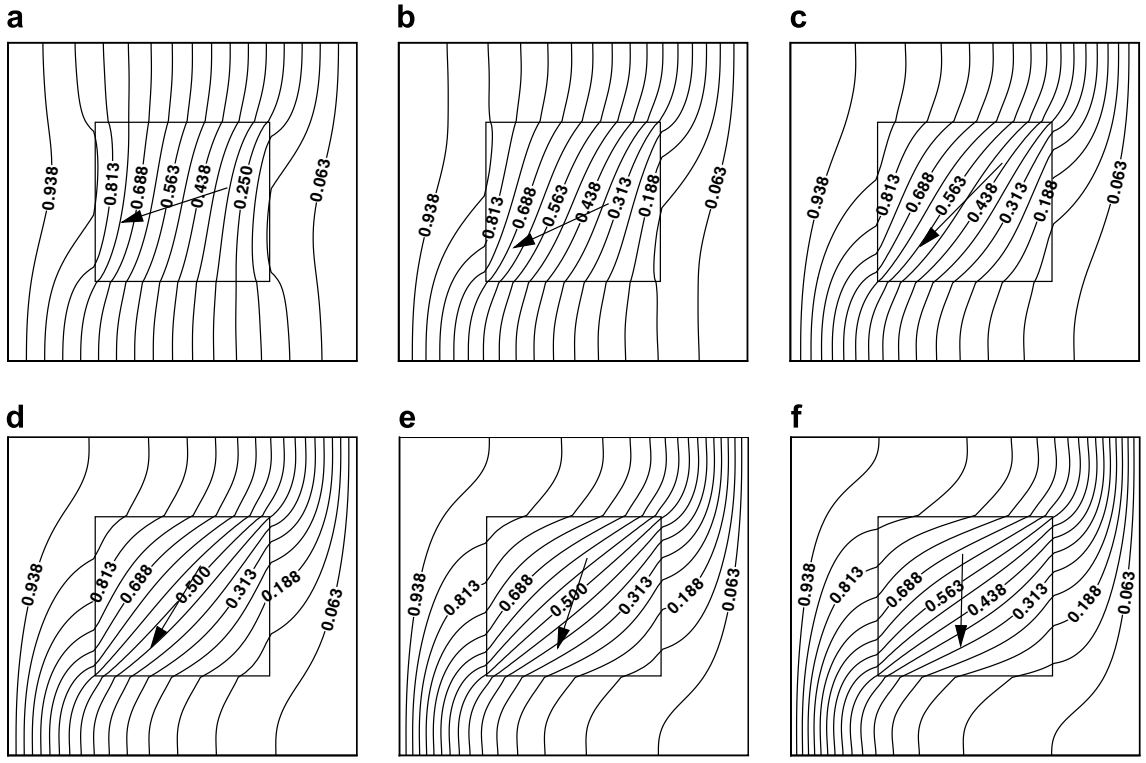

Fig. 7. The various isotherm plots for $Ra = 10^4$, $\zeta = 0.5$ and $k^* = 0.2$ beginning with an angle of inclination of 15° and in increments of 15°.

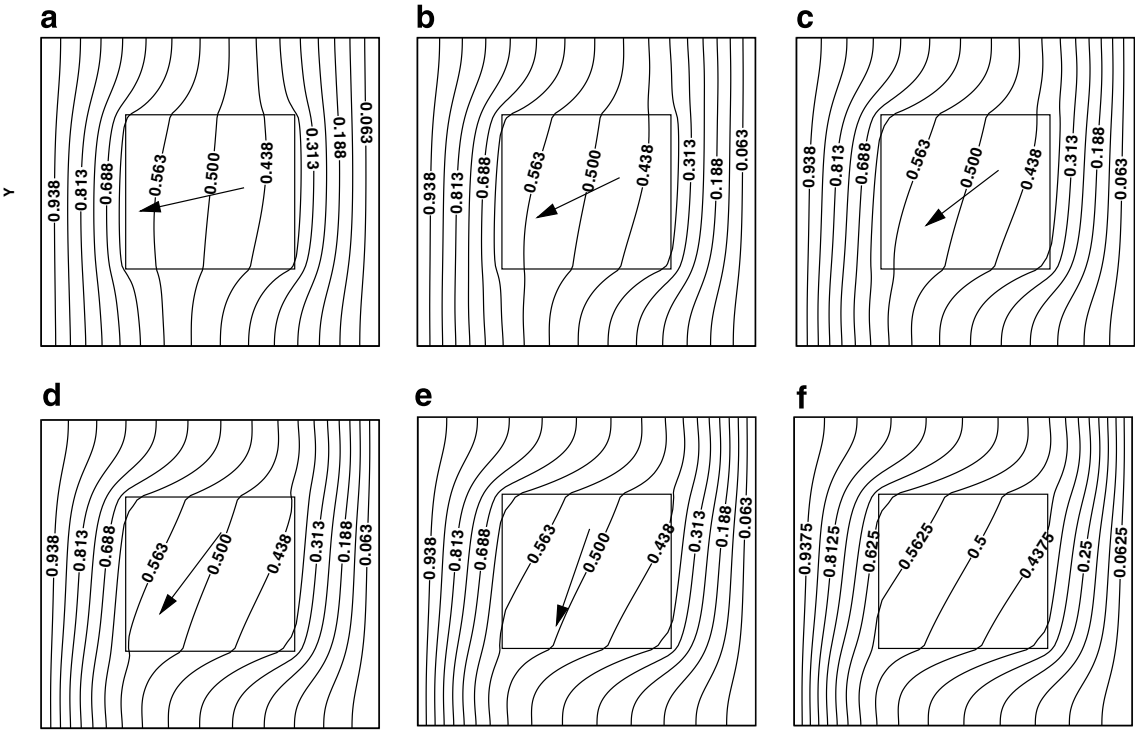

Fig. 8. The various isotherm plots for $Ra = 10^4$, $\zeta = 0.5$ and $k^* = 5.0$ beginning with an angle of inclination of 15° and in increments of 15°.

the momentum equations being u and v, respectively. In this way the velocities u and v are set to zero in the solid domain.

The energy equation in the domain is solved using two separate energy equations for fluid and solid region maintaining the flux continuity at the solid block and fluid interface. It is maintained by solving the energy equation using the Tri-Diagonal Matrix Algorithm (TDMA) with sweep in both directions. In this way the flux continuity condition in x direction is satisfied during the y sweep and vice versa.

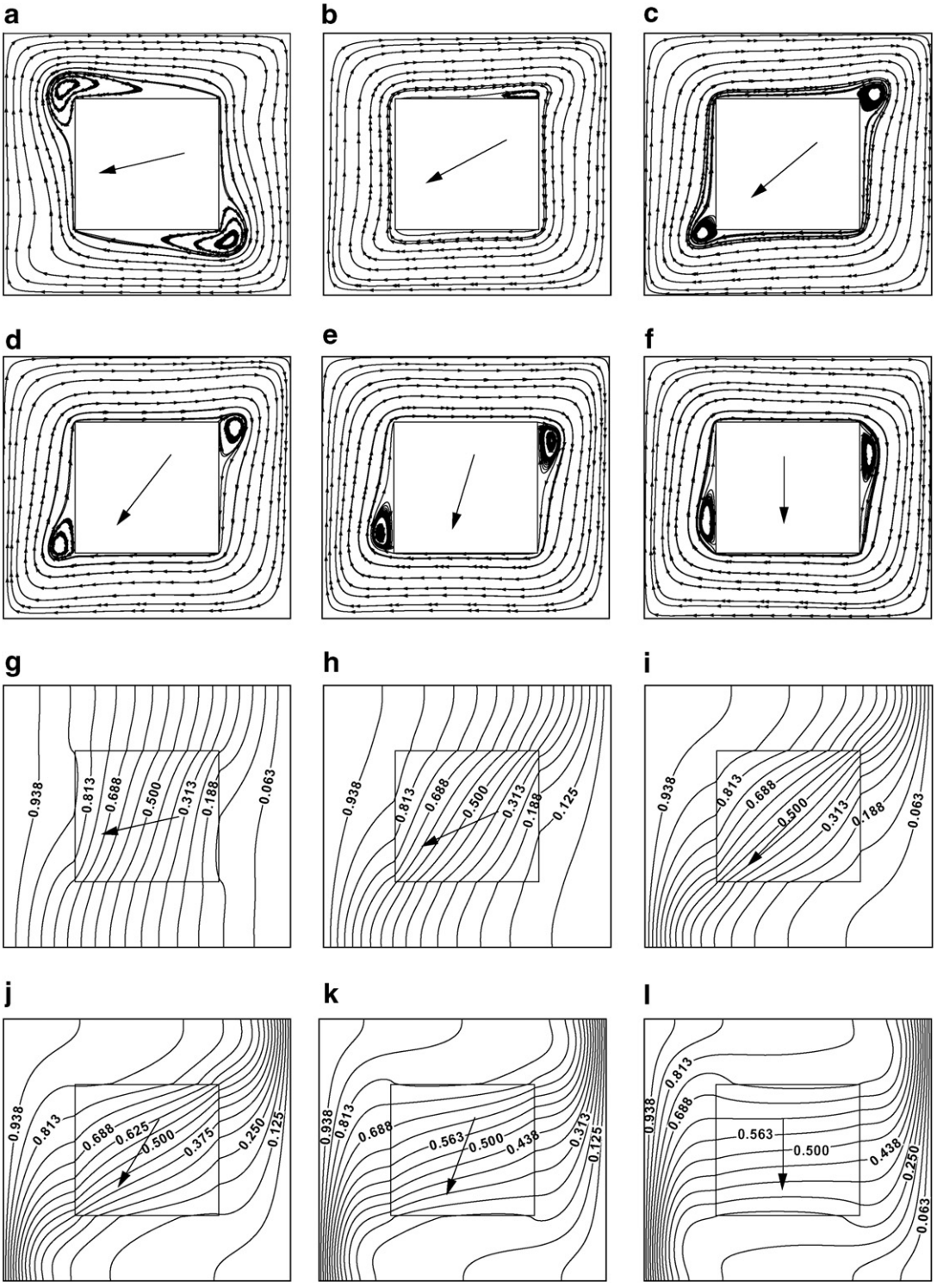

Fig. 9. The various streamline ((a)–(f)) and isotherm ((g)–(l)) plots for $Ra = 10^5$, $\zeta = 0.5$ and $k^* = 0.2$ beginning with an angle of inclination of 15° and in increments of 15°.

Also, the matching conditions at the solid/fluid interface are simultaneously satisfied. The algorithm ensured the continuity of fluxes at all control surfaces. The abrupt changes in the properties (k^* and Pr) are dealt with using the harmonic mean formulation as suggested in Patankar [11] and House et al. [4].

The TDMA [11] is applied for the line-by-line solution of the momentum, energy and pressure correction equations. The pseudo-transient approach is followed for the numerical solution as it is useful for situation in which governing equations give rise to stability problems e.g. buoyant flows [13]. The iterative procedure is initiated by the solution of

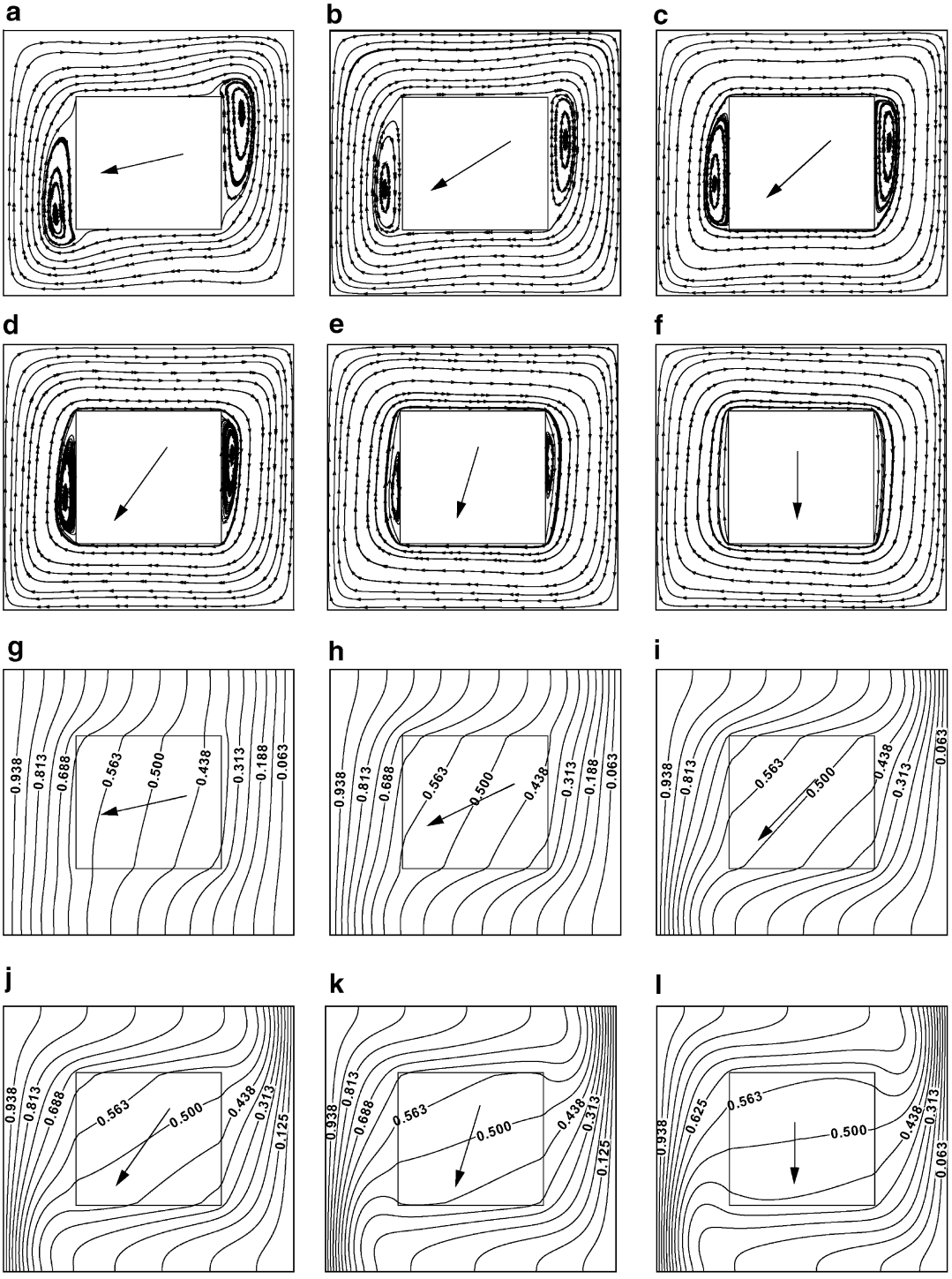

Fig. 10. The various streamline ((a)–(f)) and isotherm ((g)–(l)) plots for $Ra = 10^5$, $\zeta = 0.5$ and $k^* = 5.0$ beginning with an angle of inclination of 15° and in increments of 15°.

energy equation followed by momentum equations and is continued until convergence is achieved. Euclidean norm of the residual is taken as convergence criteria for each dependent variable in the entire flow field [14]. Mass convergence criteria was taken as 10^{-6} and temperature convergence was taken as 10^{-4}. The value of ζ can be varied for different conductivity ratios (k^*) and different Rayleigh numbers (Ra) and the effect on the heat transfer rate can be studied by calculating the Nusselt number. The calculated numerical results were then validated with the results of House et al. [4]. In the present study numerical results were calculated for various body sizes and various k^* values.

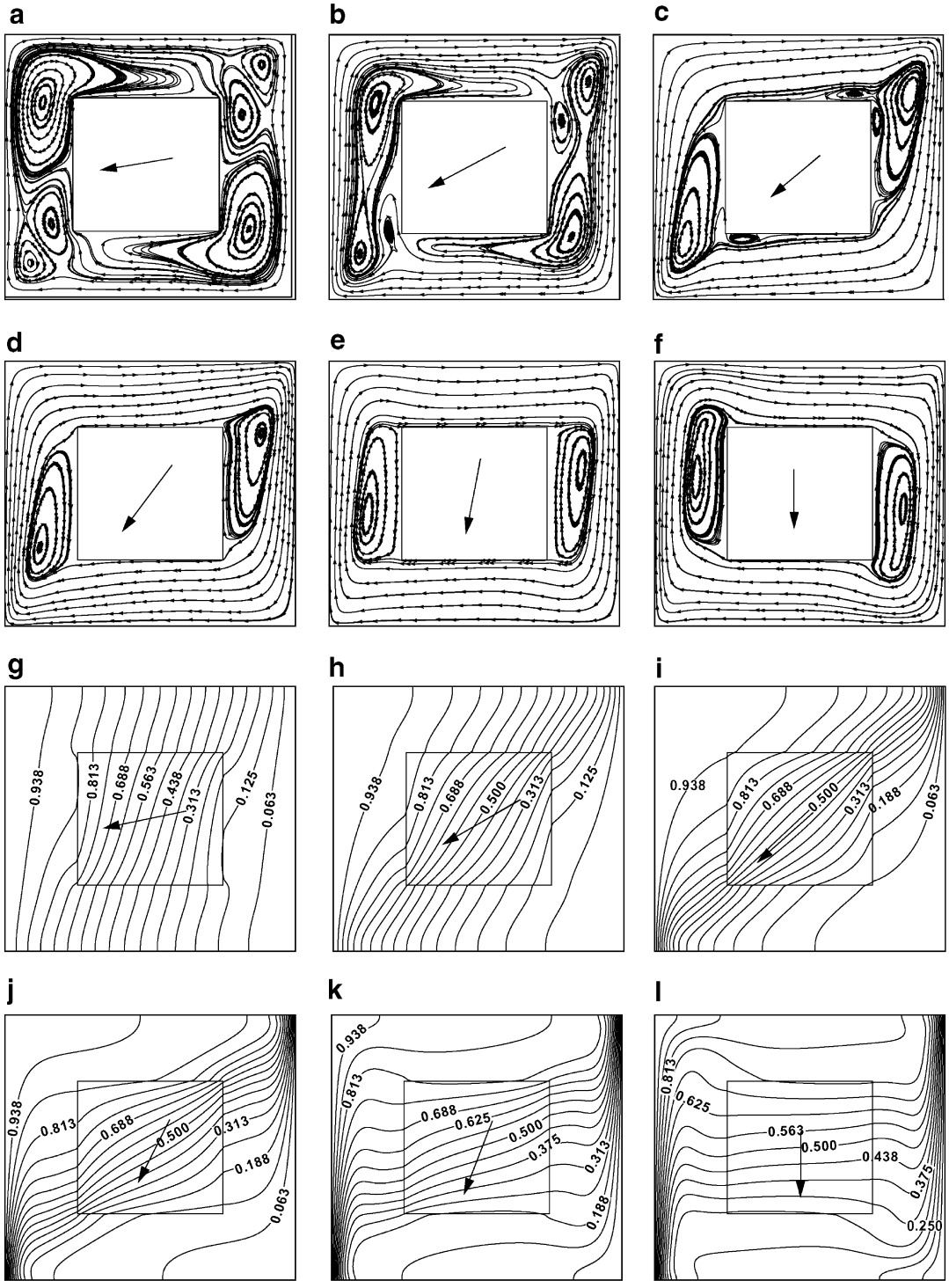

Fig. 11. The various streamline ((a)–(f)) and isotherm ((g)–(l)) plots for $Ra = 10^6$, $\zeta = 0.5$ and $k^* = 0.2$ beginning with an angle of inclination of 15° and in increments of 15°.

5. Grid independence study

Control volumes were developed such that there were more number of control volumes between body and the enclosing wall. In every direction the number of control volumes was such that there were NCV1 control volumes between body and the wall, NCV2 in the body and NCV1 again between wall and the body. A typical computational grid is shown in Fig. 2. First, grid independent study was done for various grid sizes of

(1) NCV1 = 22 and NCV2 = 20
(2) NCV1 = 27 and NCV2 = 25
(3) NCV1 = 30 and NCV2 = 28

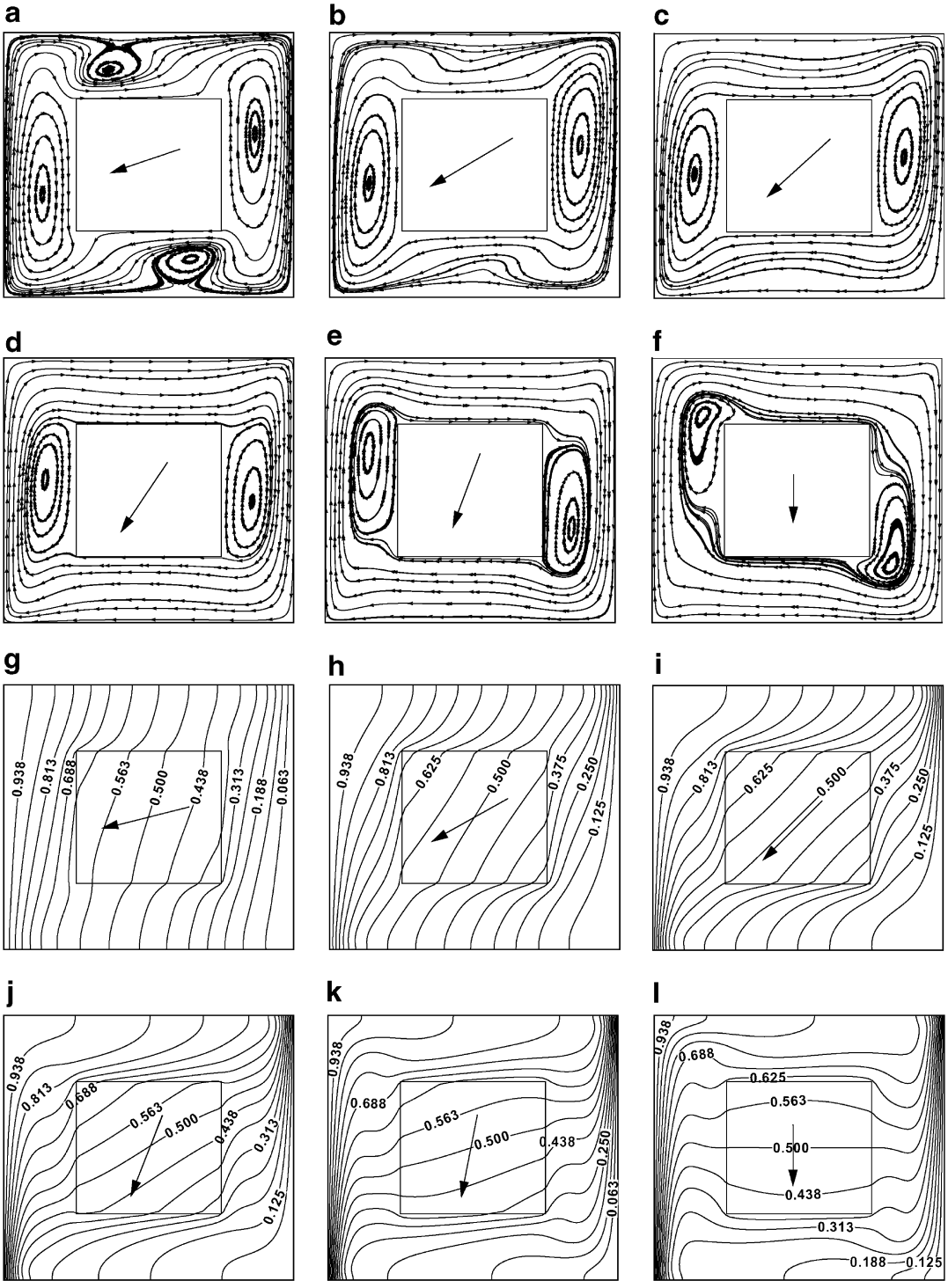

Fig. 12. The various streamline ((a)–(f)) and isotherm ((g)–(l)) plots for $Ra = 10^6$, $\zeta = 0.5$ and $k^* = 5.0$ beginning with an angle of inclination of 15° and in increments of 15°.

for a ζ value of 0.5 and for $Ra = 10^5$ and different k^* values of 0.2 and 5.0.

Table 1 shows the grid independence test results. It is found that for a grid size of NCV1 = 27 and NCV2 = 25 and beyond that there was not much improvement in the numerical results. The change in the Nusselt number occurred only at the second and third decimal points. Hence this grid size is used throughout the computation.

6. Validation of the code

Extensive validation of the developed code has been carried out by comparing the results with those of House et al. [4]. The average Nusselt number has been computed for various ζ with $k^* = 0.2$ and 5.0. The same has been performed for $Ra = 10^3$, 10^4, 10^5 and 10^6 and are shown in Fig. 3(a–d), respectively. Excellent agreement has been obtained. The computations have been performed by varying k^* and Nu_{avg} for $Ra = 10^5$ and $\zeta = 0.5$ and is shown in Fig. 4. In this case also, good agreement has been obtained. Details of the grid independence and validation of the code may be obtained in Reddy [15].

7. Results and discussion

The calculated flow fields are plotted for angle of inclination varying from 15° to 90° in steps of 15° for Ra varying from 10^3–10^6 and for k^* values of 0.2 and 5.0 . The Pr of the fluid considered is 0.71 (air).

Case (a): $Ra = 10^3$

Figs. 5 and 6 show the isotherms for various angle of inclination, for $k^* = 0.2$ and $k^* = 5.0$, respectively. The streamlines (not shown here) has a closed circular path as the Ra is small and conduction is the mode of heat transfer. When the isotherms for these two cases are compared, it is observed that for higher k^* values (Fig. 6), the isotherms

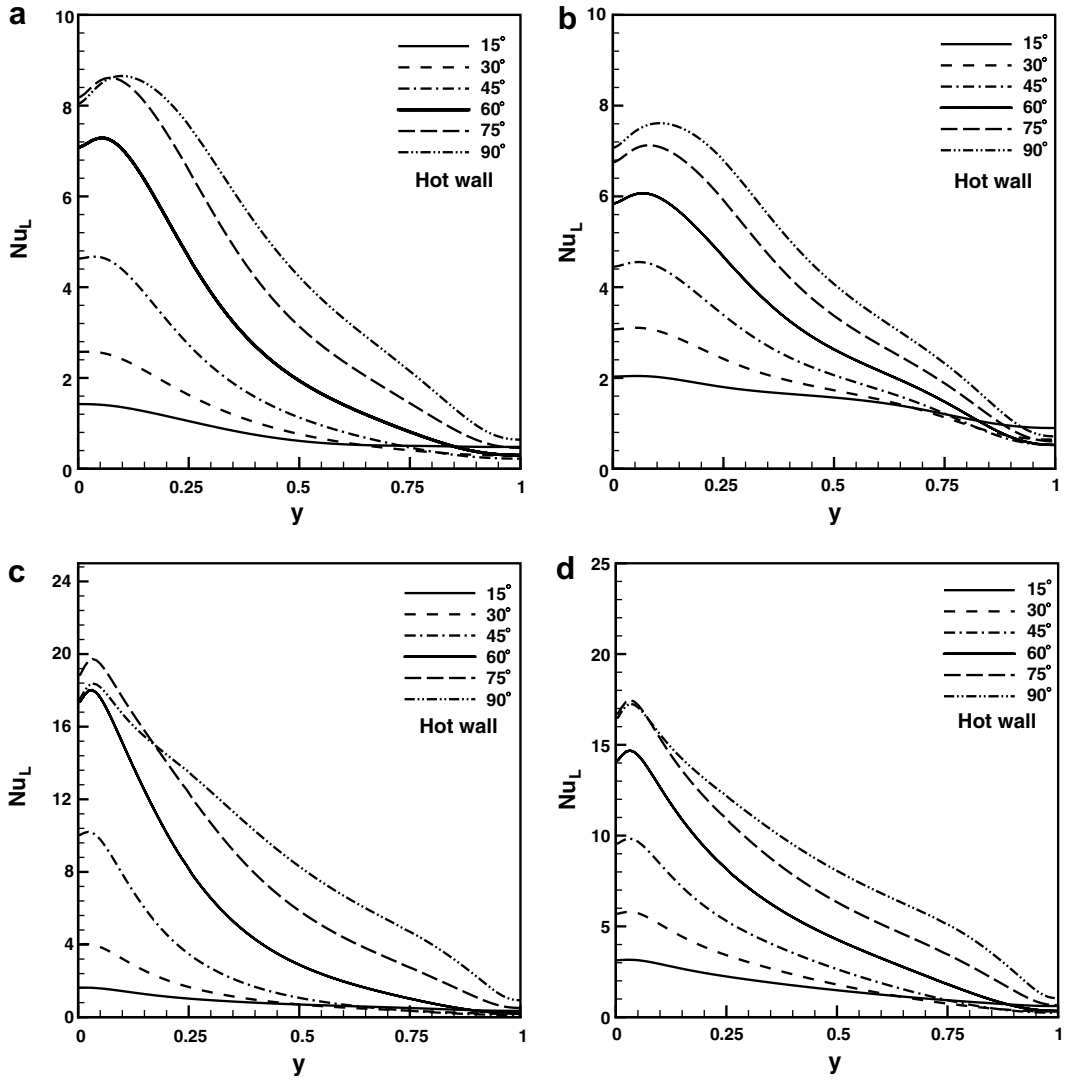

Fig. 13. The local Nusselt number plots for $\zeta = 0.5$ beginning with an inclination angle of 15° and in increments of 15° (a) $Ra = 10^5$ and $k^* = 0.2$ (b) $Ra = 10^5$ and $k^* = 5.0$ (c) $Ra = 10^6$ and $k^* = 0.2$ (d) $Ra = 10^6$ and $k^* = 5.0$.

are clustered near the isothermal walls indicating that heat transfer is more compared to low k^* value of 0.2 (Fig. 5). The isotherm patterns remain unaltered by the angle of inclination. The Nu_{avg} is higher for $k^* = 5.0$ compared to $k^* = 0.2$ as shown in Fig. 14(a). The Nu_{avg} also remains constant with ϕ confirming conduction is the mode of heat transfer. At $Ra = 10^3$, natural convection flow is significantly suppressed. The high value of k^* allows for higher diffusion heat transfer. Thus the average Nusselt number for $k^* = 0.2$ is less than for $k^* = 5.0$ at all angles.

Case (b): $Ra = 10^4$

It is observed that the stream lines patterns (not shown) are almost uniform signifying the relative dominance of diffusion even at this stage. As the angle (ϕ) increases, the concentration of isotherms at the corners of the isothermal walls of the block i.e. bottom (left) and top (right) increase showing that significant heat transfer occurs across these corners due to less thermal resistance (see Figs. 7 and 8). The wavy pattern and the clustering of the isotherms indicate that advection process has begun and this increases with the increase in the angle. Most of the heat transfer on the hot wall occurs at the bottom. Even at low angle of inclination, for $k^* = 5.0$, the isotherms are concentrated near the hot and cold walls compared to $k^* = 0.2$ indicating that heat transfer is more. From Fig. 14(b) it is seen that the average Nusselt number for $k^* = 0.2$ is less than that of $k^* = 5.0$ up to an angle of 86°, where they are equal and beyond that the average Nusselt number for $k^* = 0.2$ is slightly greater than $k^* = 5.0$. This range where they are equal has been termed as "critical angle".

Case (c): $Ra = 10^5$

As Ra is increased to 10^5 (Figs. 9 and 10), streamline patterns show regions of flow separation. The size of the vortex formed is large for small angle of inclination and the size reduces for higher angles. The development and shifting of the two corner vortices on the body with increase in angle is well captured for $k^* = 0.2$. However, for $k^* = 5.0$, the size of the vortex formed decreases with the increase in angle and finally disappears for $\phi = 90°$ (Fig. 10). For a high thermal conductivity body, the recirculation region tends to distribute the temperature effectively. With the increase in angle the wall thermal boundary layer thickness increases at the isothermal wall side of the enclosure. The heat transfer across the block appears to be one dimensional from the upper passage to the lower passage. The Nu_L is plotted along the isothermal hot wall for various angle of inclination and shown in Fig. 13(a) and (b). Increase in the angle of inclination results in the increase of Nu_L. Higher k^* means better conductive heat transfer within the core. That is why the relative Nu_L value is more for higher k^* value at lower angle of inclination. With similar reasoning as given for Case (b), Nu_{avg} is higher for $k^* = 5.0$ compared to $k^* = 0.2$ for low angle of inclination as seen in Fig. 15(a). As the angle increases, the trend reverses. The average Nusselt number for $k^* = 0.2$ is more than the average Nusselt number for $k^* = 5.0$ beyond 67.9°. Two vortices noticed at 90° inclination for $k^* = 0.2$ may have thus increased the convective heat transfer compared with $k^* = 5.0$. At higher angle of inclination, for $k^* = 0.2$ (Fig. 9(l)), the isotherms in the block imply that the direction of heat transfer is in the direction of the adiabatic walls. That means no heat transfer takes place in the differentially heated walls. This makes the thermal boundary layer dense near the isothermal walls and increase the Nu_{avg} value.

Case (d): $Ra = 10^6$

As observed from Figs. 11 and 12, for $k^* = 0.2$ and smaller ϕ, more number of vortices with complex stream line pattern are evolved. This could be due to the reason that at low k^* and high Ra, the advecting fluid has higher temperature resulting in large buoyancy forces which leads to the formation and break up of vortices at the corners. As the angle of inclination increases, the number of such regions decrease and a few large vortices can be seen at the left and right walls of the conducting block. However, for a large k^* value, the streamlines are more organized with final settlement of two vortices on the walls of the block. For $k^* = 0.2$, as the angle of inclination increases, the thickness of the thermal boundary layer on the hot wall

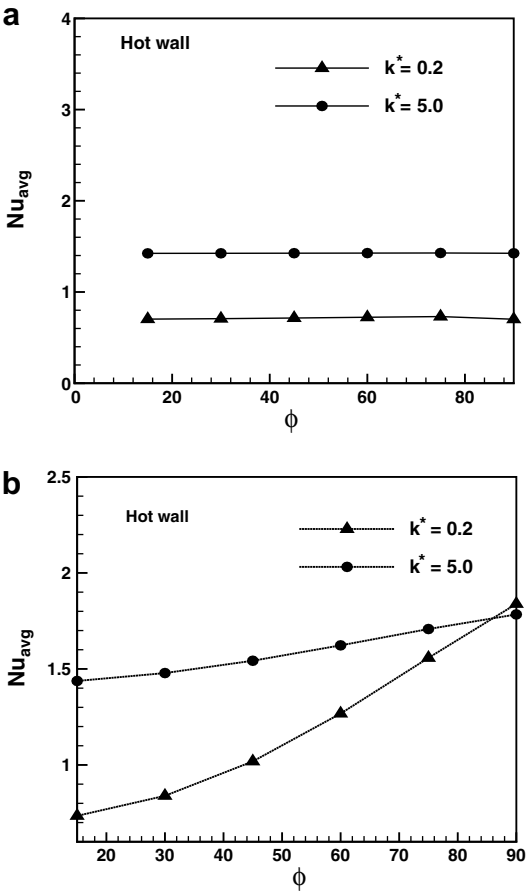

Fig. 14. The average Nusselt number plots for $\zeta = 0.5$ beginning with an inclination angle of 15° and in increments of 15° for (a) $Ra = 10^3$ and (b) $Ra = 10^4$.

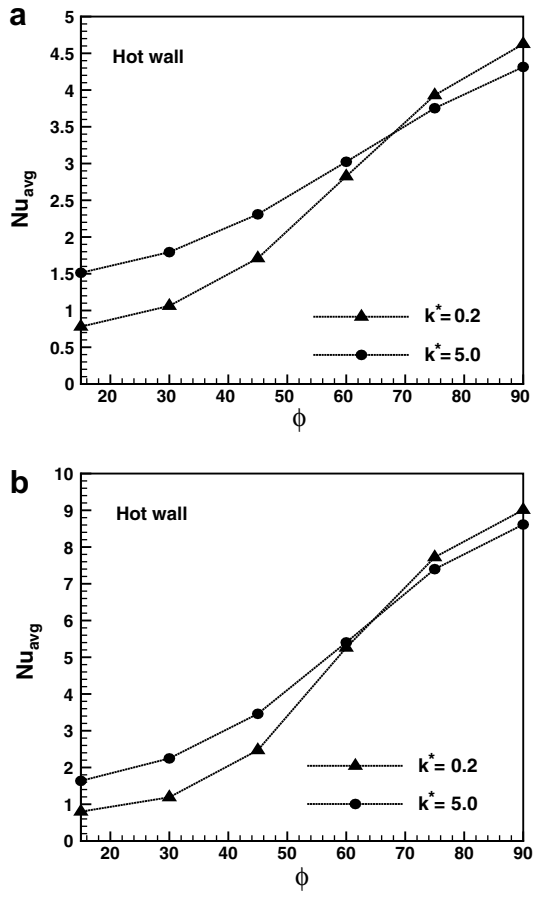

Fig. 15. The average Nusselt number plots for $\zeta = 0.5$ beginning with an inclination angle of 15° and in increments of 15° for (a) $Ra = 10^5$ and (b) $Ra = 10^6$.

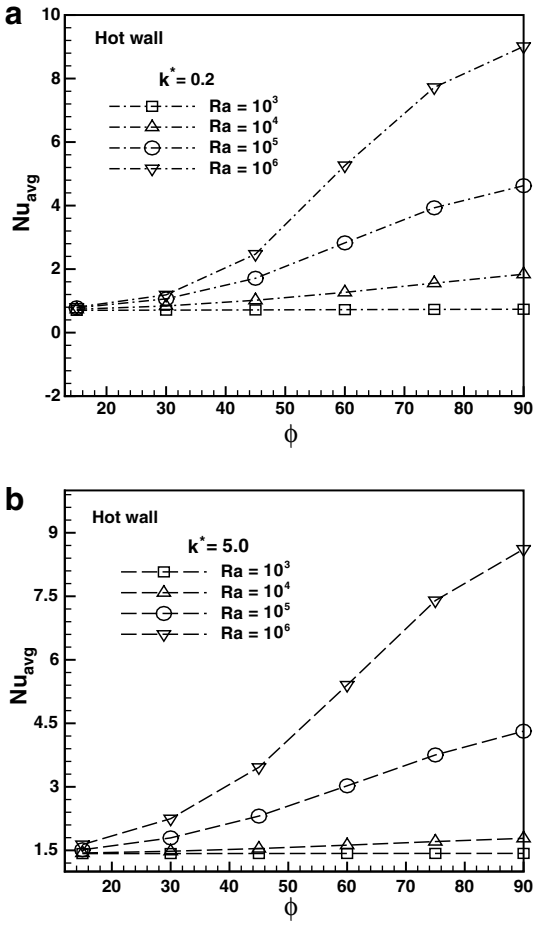

Fig. 16. The average Nusselt number plots for various Rayleigh numbers and $\zeta = 0.5$ beginning with an inclination angle of 15° and in increments of 15° for (a) $k^* = 0.2$ and (b) $k^* = 5.0$.

of the enclosure increases resulting in more heat transfer. Isotherms in the fluid region are more oriented towards the flow direction indicating the dominance of advection. The Nu_L distribution for $k^* = 0.2$ and 5.0 are shown in Fig. 13(c) and (d). The patterns are similar to Case (c) and same reasoning applies here also. From Fig. 15(b) the average Nusselt number for $k^* = 0.2$ is less than the average Nusselt number for $k^* = 5.0$ till an angle (ϕ) of 64.6° and beyond that the average Nusselt number for $k^* = 0.2$ is higher than for $k^* = 5.0$.

Effect of angle of inclination (ϕ)

Fig. 16(a) and (b) shows the variation of Nu_{avg} as a function of (ϕ) for various Ra with $k^* = 0.2$ and $k^* = 5.0$, respectively. It is observed that for $Ra = 10^3$, Nu_{avg} remains constant for the range of (ϕ) considered indicating that conduction is the mode of heat transfer. For $\phi = 0$, the imposed thermal boundary condition is that of a thermally stratified fluid. Therefore, with an increase in angle ϕ, Nu_{avg} increases significantly. For low $\phi = 15°$, Nu_{avg} for all Ra number considered are nearly equal in both the cases. With increase of Ra, convection is the dominant mode of heat transfer which results in a significant increase in Nu_{avg}.

8. Conclusions

Natural convection conjugate heat transfer inside an inclided square cavity with an internal conducting block has been carried out with $\zeta = 0.5$ for different Rayleigh number from 10^3 to 10^6 and conductivity ratio values of $k^* = 0.2$ and $k^* = 5.0$. The following conclusions are made:

- Up to $Ra = 10^3$, conduction is the mode of heat transfer. Above this Ra, convection mode of heat transfer begins to dominate.
- Above $Ra = 10^3$, there exists a critical point where the Nu_{avg} value for low and high k^* cases interchange relative magnitude.
- Below critical point, a body with higher k^* value assists in higher heat transfer.
- It can be concluded that a body with low k^* can transfer more heat than a body with high k^* beyond the critical point.
- At low Rayleigh numbers angle of inclination has nominal effect on heat transfer for different k^*.

References

[1] S. Ostrach, Natural convection in enclosures, J. Heat Transfer, 50th Anniversary Issue 110, 4-B, 1988, pp. 1175–1190.

[2] D.M. Kim, R. Viskanta, Study of the effects of wall conductance on natural convection in differentially oriented square cavities, J. Fluid Mech. 144 (1984) 153–176.

[3] G. de Vahl Davis, Natural convection of air in a square cavity: a bench mark solution, Int. J. Numer. Methods Fluids 3 (1983) 249–264.

[4] J.M. House, C. Beckermann, T.F. Smith, Effect of a centered conducting body on natural convection heat transfer in an enclosure, Numer. Heat Transfer 18 (1990) 213–225.

[5] S.B. Sathe, Y. Joshi, Natural convection arising from a heat generating substrate-mounted protrusion in a liquid-filled two-dimensional enclosure, Int. J. Heat Mass Transfer 34 (1991) 2149–2163.

[6] Y.S. Sun, A.F. Amery, Effects of wall conduction, internal heat sources and an internal baffle on natural convection heat transfer in a rectangular enclosure, Int. J. Heat Mass Transfer 40 (1997) 915–929.

[7] Y. Liu, N.P. Thien, A complete conjugate conduction convection and radiation problem for a heated block in a vertical differentially heated square enclosure, Comput. Mech. 24 (1999) 175–186.

[8] M.Y. Ha, M.J. Jung, A numerical study on three-dimensional conjugate heat transfer of natural convection and conduction in a differentially heated cubic enclosure with a heat-generating cubic conducting body, Int. J. Heat Mass Transfer 43 (2000) 4229–4248.

[9] N. Yucel, H. Ozdem, Natural convection in partially divided square enclosures, Heat Mass Transfer 40 (2003) 167–175.

[10] M.Y. Ha, I.-K. Kim, H.S. Yoon, K.S. Yoon, J.R. Lee, S. Balachandar, H.H. Chun, Two-dimensional and unsteady natural convection in a horizontal enclosure with a square body, Numer. Heat Transfer: Part A 41 (2002) 183–210.

[11] S.V. Patankar, Numerical Heat Transfer and Fluid Flow, Hemisphere publication Co., NY, 1980.

[12] T. Hayase, J.A.C. Humphrey, R. Greif, A consistently formulated QUICK scheme for fast and stable convergence using finite-volume iterative calculation procedures, J. Comput. Phys 98 (1992) 108–118.

[13] H.K. Versteeg, W. Malalasekera, An Introduction to Computational Fluid Dynamics: the Finite Volume Method, Longman Group Ltd., Malaysia, 1995.

[14] J.P.V. Doormaal, G.D. Raithby, Enhancements of the SIMPLE method for predicting incompressible fluid flows, Numer. Heat Transfer 7 (1984) 147–163.

[15] K.S.K. Reddy, Study of natural convection in a cavity with an internal conducting block, Master's thesis, Department of Mechanical Engineering, Indian Institute of Technology Guwahati, India, July 2005.